



Micro/Nanofluidic Device for Single-Cell-Based Assay

Kwang-Seok Yun* and Euisik Yoon

Department of Electrical Engineering and Computer Science (Division of Electrical Engineering), Korea Advanced Institute of Science and Technology (KAIST), 373-1 Guseong-dong, Yuseong-gu, Daejeon 305-701, Korea
E-mail: ksyun@iml.kaist.ac.kr

Abstract. In this paper we have proposed and demonstrated a microfluidic device for a fast and parallel single-cell based assay. The proposed device is designed to passively capture single-cells or beads on multiple cell-positioning sites by a pre-defined fluidic stream and inject specific reagents or drugs onto each isolated single-cell. The device consists of surface-modified silicon channels capped with a grooved polydimethylsiloxane (PDMS) cover layer. A cell capture experiment has been performed using polystyrene beads as well as CHO DG44 living cells, and successful positioning of a single-cell on the cell-positioning sites was achieved. Also, we have demonstrated independent drug injection into a specific target cell.

Key Words. lab-on-a-chip, single-cell analysis, cell capture, drug screening, surface modification

1. Introduction

Performing fundamental life functions, the cell is functionally and structurally the basic unit of all living creatures. Most living cells grow and divide with creating or consuming components such as proteins, ions, and other molecules. Such cellular functions can be controlled using external chemicals such as drugs or other reagents. Specifically, the cell transduces binding events with some drug candidates or reagents and provides quantitative information on the stimulation.

Cells that are in the target of monitoring generally coexist with other cells, and therefore are exposed to a mixture of proteins, ions, and neurotransmitters released from neighboring cells. Thus, dynamic monitoring of a single-cell in an independently controlled environment without the influence of neighboring cells is important for individual cell analysis.

As technology has advanced, the capabilities and sensitivity of cellular studies have been greatly improved. Current techniques allow the examination of single-cell characteristics either *in vivo* or *in vitro*, which makes possible the application of cell-based functional assays to not only research of cellular function but also new drug development. With recent rapid growth in biotechnology, bioinformatics, and bioengineering, many origins of diseases have been studied and numerous drug candidates have been designed and developed. Thereupon, it is necessary to rapidly screen the toxicity, effectiveness, and

other aspects of the designed drug candidates with live cells.

Previously, single-cells have been manually loaded on a capillary end for capillary electrophoresis (Tong and Yeung, 1997; Krylov and Dovichi, 2000) or manually isolated using a micromanipulator (Bratten et al., 1998). In these cases, only a few cells can be analyzed at a time, and as such it is difficult to monitor many cells in a short time. Other researchers have used cells cultured on a microelectrode (Aebischer et al., 1996; Jimbo et al., 1993). Thielecke et al. reported a single-cell positioning chip that places single-cells on ring electrodes by suction of a vacuum pump (Thielecke et al., 1999). However, with this procedure, it is difficult to independently control the environment of each cell located in the individual ring electrode structure. Recently, increased progress in microfluidic and microfabrication technology has greatly improved the manipulation of fluids and cells in microfluidic devices (Daridon et al., 2002; Wheeler et al., 2002; Manaresi et al., 2003; Ozkan et al., 2003; Huang et al., 2003).

In this paper, we propose a high-throughput single-cell analysis system, which has the capability of single-cell monitoring and drug screening, and report experimental results obtained using the fabricated device for single-cell capturing and nanoliter drug injection.

2. Microfluidic Chip for Single-Cell Capture and Nanoliter Drug Injection

For single-cell assays, it is necessary to isolate single-cells in a specific cell capturing site or a micro-reactor. In this work, we have adopted passive cell manipulation and isolation into cell capturing sites. Figure 1 shows a schematic top-view of the proposed structure. The cell suspension media is introduced into the inlet by external pressure and a single cell is passively positioned on each cell-positioning site. For efficient capture of the cell, each cell-positioning site is designed to have a hook-shape and a narrow drain channel where media can flow while cells are blocked. Once a cell is captured, it blocks the flow

*Corresponding author.

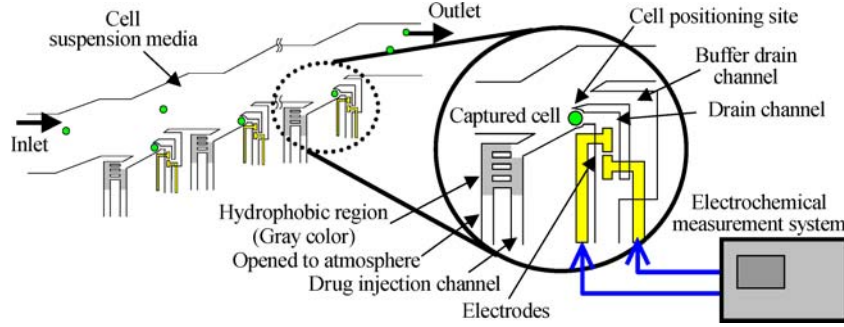


Fig. 1. Schematic illustration of proposed structure.

through the drain channel and prevents other cells from being captured. A drug or other chemicals can be injected on each captured cell through the corresponding injection channels. A hydrophobic region is formed to prevent the suspension media from flowing out. This hydrophobic channel also allows air to leak out during drug introduction. A buffer drain channel near the cell-positioning site is prepared to drain overflowed drug and prevent mixing of the injected drug with the main suspension media.

3. Microchannel Design

For the proposed device, two types of channels are required—one hydrophilic and the other hydrophobic. As shown in Figure 1, most regions of the flow channel are hydrophilic for easy filling of sample solutions, including cell suspension media and drug candidates. The hydrophobic channel is required for air leak-out during the merging process of two fluids. During the drug injection step, the air filled in the drug injection channel leaks out to the atmosphere through the hydrophobic channel region. This prevents air introduction into the main channel, which could cause a critical failure in the device operation.

3.1. Capillary force in micromachined microchannel

In many cases, micromachined microchannels are rectangular channels, as shown in Figure 2. Three walls have the same surface material with the same contact angles, while only one side is comprised of a different material with a different contact angle. Then, the total energy of the capillary channel in Figure 2 is expressed as

$$E_s = 2xh\gamma_{s2l} + xw\gamma_{s2l} + xw\gamma_{s1l} + 2(L-x)h\gamma_{s2a} + (L-x)w\gamma_{s2a} + (L-x)w\gamma_{s1a}; \quad (1)$$

where γ is surface energy per unit area. By Young's law, the equation can be written in terms of contact angles

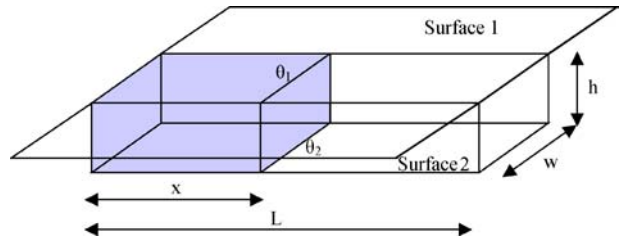


Fig. 2. Schematic view of micromachined rectangular microchannel. Three walls have the same surface material with the same contact angle (θ_2), while only one side is comprised of a different material with a different contact angle (θ_1).

as below.

$$E_s = -(2xh\gamma_{la} \cos \theta_2 + xw\gamma_{la} \cos \theta_2 + xw\gamma_{la} \cos \theta_1) + 2Lh\gamma_{s2a} + Lw\gamma_{s2a} + Lw\gamma_{s1a} \quad (2)$$

Taking the derivative of equation (2) with respect to x , we obtain the equivalent force F applied on the capillary fluid column along the x direction.

$$F = -\frac{dE_s}{dx} = 2h\gamma_{la} \cos \theta_2 + w\gamma_{la} \cos \theta_2 + w\gamma_{la} \cos \theta_1 = \Delta P_{la} \cdot w \cdot h \quad (3)$$

Therefore, the pressure drop across the liquid-air interface is expressed as;

$$\Delta P_{la} \approx \left(\frac{2}{w} + \frac{1}{h}\right)\gamma \cos \theta_2 + \frac{1}{h}\gamma \cos \theta_1 \quad (4)$$

As shown in equation (4), the capillary force is a function of the channel dimension and contact angles. When the polarity of equation (4) is positive, the channel is hydrophilic and will introduce absorbing capillary force for water. Otherwise, the channel will be hydrophobic for negative capillary force in equation (4), having repelling force for water. Utilizing this phenomenon, we have designed

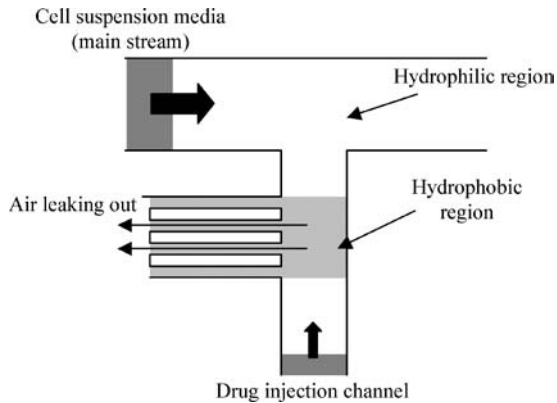


Fig. 3. Schematic drawing of the drug injection structure for the proposed single-cell analysis chip. Gray region is hydrophobic channel and other regions are all hydrophilic.

a structure to allow air leakage during drug introduction into the main stream.

3.2. Merge of two liquids with air leaking out

Previously, a gas bubble filter utilizing structural changes of microchannels was reported for filtering out gas bubbles in microchannels (Tsai and Lin, 2001). We have used surface modification and geometrical modification to induce air leakage during the merging of two liquids. This is particularly important for drug introduction into the main stream of cell suspension media. Figure 3 provides a schematic drawing of the drug injection structure. In the figure, the gray region is hydrophobic and the other regions are all hydrophilic. The cell suspension media is stopped at the boundary of the hydrophobic region. The drug is subsequently introduced through the drug injection channel and is also thereafter stopped at the boundary of hydrophobic region. During the drug introduction, the air occupying the injection channel leaks out through the narrow hydrophobic channels. Finally, with increased injection pressure, the drug is injected into the cell suspension media, passing through the hydrophobic region.

3.3. Implementation of microchannel

Figure 4 provides a schematic view of the microchannels designed in this work. The hydrophilic microchannel is formed with polydimethylsiloxane (PDMS) and silicon dioxide, as shown in Figure 4(a). In this case, three walls are comprised of PDMS with a measured contact angle of about 97° while the other side is silicon dioxide with a contact angle of about 45° . The microchannel was designed to have a channel height of $20\ \mu\text{m}$ so that cells (generally smaller than $15\ \mu\text{m}$ in diameter) can flow through the channel. In this case, the capillary force can be calculated as a function of channel width from equa-

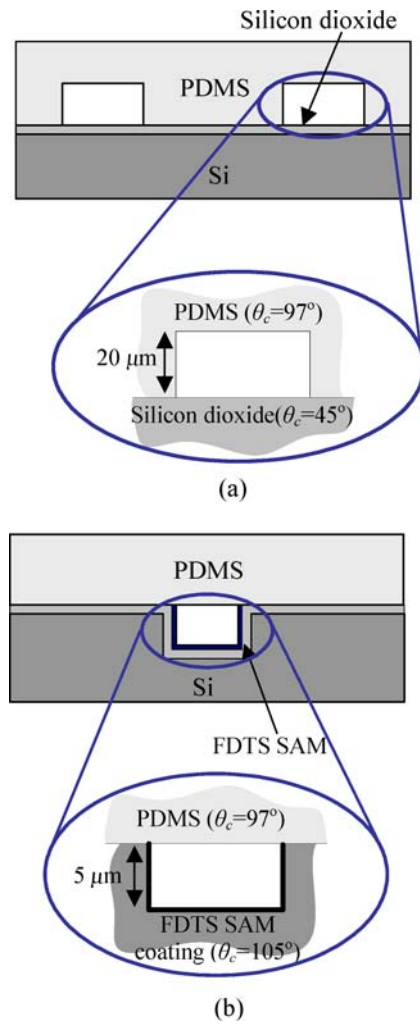


Fig. 4. Cross-sectional view of proposed microchannels. (a) Hydrophilic microchannel composed of PDMS and silicon substrate. (b) Hydrophilic microchannel composed of PDMS and FDTD SAM coated silicon surface.

tion (4), as shown in Figure 5. The channel can be either hydrophilic or hydrophobic, depending on channel width. When the channel width is larger than $5\ \mu\text{m}$, the channel becomes hydrophilic. We have designed the minimum channel width to be larger than $10\ \mu\text{m}$ to guarantee hydrophilic microchannel formation.

The hydrophobic microchannel is formed using a PDMS and silicon surface modified by self-assembled-monolayer (SAM) coating of 1H, 1H, 2H, 2H-perfluorodecyltrichlorosilane (FDTD), as shown in Figure 4(b). The contact angle of the FDTD SAM coated surface was measured to be approximately 105° . In this case, the channel is always hydrophobic, regardless of the channel dimension, because all four walls have hydrophobic surfaces.

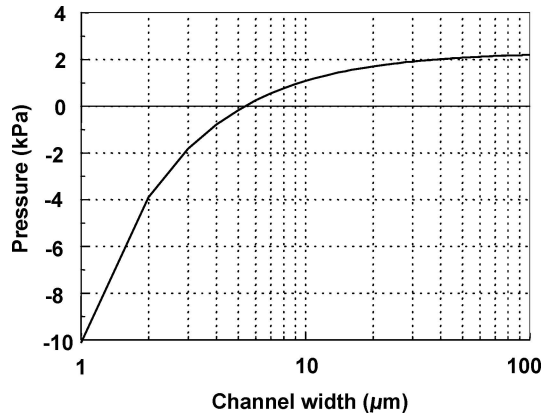


Fig. 5. Capillary force for various channel widths for a channel depth of $20\ \mu\text{m}$ in the structure of Figure 4(a).

4. Fabrication

The proposed device is composed of a grooved PDMS substrate bonded to a silicon substrate. Figure 6 shows the fabrication processes of the device. For the silicon structure, the silicon is etched using reactive-ion-etching (RIE) and a gold layer is deposited. The PECVD silicon nitride and silicon dioxide are deposited and patterned to form electrodes and pad areas. For the selective SAM coating of FDTS, first, aluminum is deposited and locally etched where the hydrophobic surface is to be formed by FDTS coating. Then, the substrate is dipped in FDTS

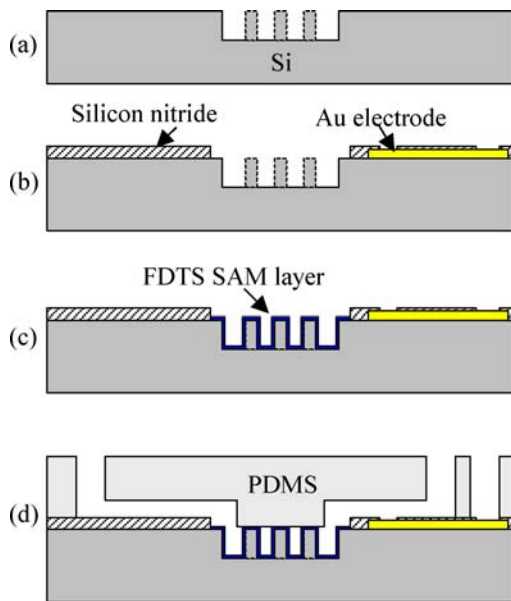


Fig. 6. Fabrication processes. (a) Silicon etch. (b) Au patterning and silicon nitride deposition. (c) FDTS SAM coating. (d) Bonding with PDMS structure.

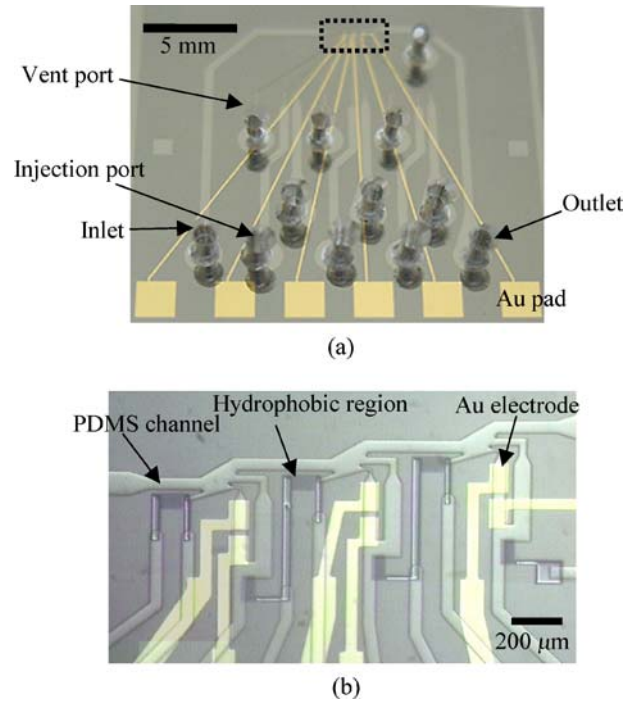


Fig. 7. (a) Photograph of the fabricated device. (b) Detailed view of the dotted region in (a).

solution, followed by aluminum etching. This leaves the FDTS SAM layer on the exposed area (Handique et al., 2000; Srinivasan et al., 1998). For the PDMS substrate, the grooved PDMS structure is formed by a replica molding method using $20\ \mu\text{m}$ -thick SU-8 (Microchem Co.) structures as a mold. Finally, the PDMS surface is modified to a hydrophilic surface using O_2 plasma treatment and is then bonded with silicon substrate. The hydrophobicity of the PDMS surface is fully recovered after one day with a contact angle of about 97° . Figure 7 shows a photograph of the fabricated device. The initial design of the devices has three cell-positioning sites. In the picture, gray regions are FDTS SAM coated hydrophobic areas.

5. Experiments and Discussion

In the experiment, the fluid stream including cell suspension media and drug injection media is controlled by external air pressure using a low-range pressure regulator. First, we tested the feasibility of cell capturing using polystyrene beads ($15\ \mu\text{m}$ in diameter) in distilled water. The hydrophilic region is gently filled with media through the inlet to the outlet. Then, the bead is introduced through the inlet by external pressure. Figure 8 shows a series of images taken during a bead capturing and drug injection experiment. As shown in Figure 8(a), a bead can be exactly

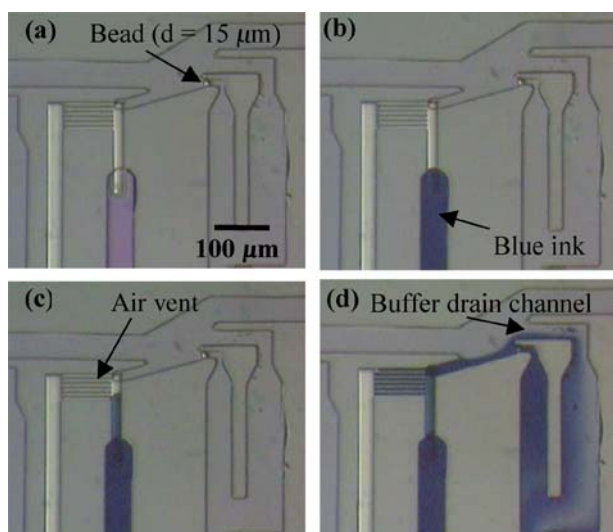


Fig. 8. Series of images during the cell-positioning test. (a) Capturing a bead. (b) Introducing blue ink (drug) from the injection channel, now stopped at the hydrophobic region. (c) Overcoming the capillary force by increasing the injection pressure. (d) Ink (drug) injection onto the captured bead.

placed on a cell-positioning site from a pre-determined flow stream. Also, this figure shows that the media does not enter the hydrophobic region, but instead is stopped at the interface of the hydrophilic and hydrophobic regions. After the bead is captured, blue ink is introduced from the injection channel. Without injection pressure, the ink is introduced through the hydrophilic injection channel until it is blocked at the entrance of the hydrophobic region (Figure 8(b)). The ink then passes through the hydrophobic region by the application of injection pressure (Figure 8(c)) and is finally injected into the captured bead

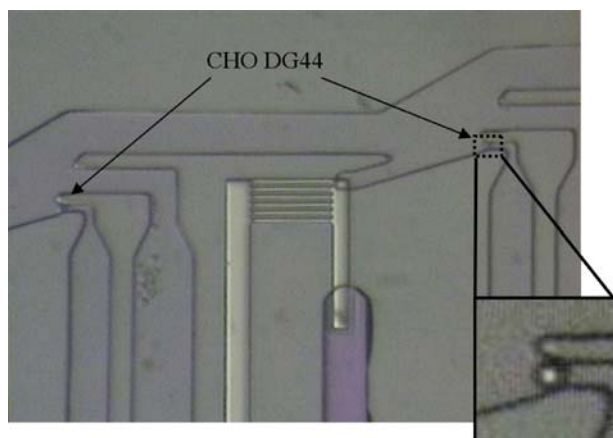


Fig. 9. Capturing of CHO DG44 cell on cell-positioning sites, with a magnified view of the captured cell.

(Figure 8(d)). During the ink injection, air in the injection channel leaks out through the hydrophobic vent channel to the atmosphere. Figure 8(d) shows that the excess ink is drained out through the buffer drain channel located above the main drain channel, demonstrating that the injected drug (in this experiment, injected ink) does not flow into other captured cells in the neighborhood.

The experiment using living cells is shown in Figure 9. This photograph shows an actual living cell, CHO DG44, captured in a cell-positioning site. The cell suspension media is phosphate buffered saline (PBS) solution.

6. Conclusions

In this paper, we have proposed and implemented a single-cell-based assay device for fast and parallel single-cell monitoring and high-throughput drug screening. The proposed single-cell assay device is designed so that a single-cell is autonomously captured in a cell-positioning site by a pre-defined fluid stream. Specific liquid including drugs or reagents can be supplied to each single-cell through a drug injection channel. A cell capture experiment has been performed using polystyrene beads and CHO DG44 cells, demonstrating successful positioning of single-cells on each cell-positioning site. Also, a simulated drug (ink) has been successfully injected into a target cell without any air introduction.

Acknowledgments

This research has been supported by the Intelligent Microsystem Center, which carries out one of the 21st century's Frontier R&D Projects sponsored by the Korea Ministry of Commerce, Industry and Energy. This work was supported by Brain Korea 21 Project, the School of Information Technology, KAIST in 2004. Also, this work has been partially supported by KOSEF through the MICROS center at KAIST.

References

- P. Aebischer, H.J. Buhlmann, M. Dutoit, L. Giovannardi, and S.A. Makohliso, "A biomimetic materials approach towards the development of a neural cell-based biosensor," in *Proc. of the 18th Annu. Int. Conf. of the IEEE Eng. in Med. and Biol. Soc.*, edited by IEEE Engineering in Medicine and Biology (IEEE, Amsterdam, The Netherlands, 1996), p. 81.
- C.D.T. Bratten, P.H. cobbold, and J.M. Cooper, *Anal. Chem.* **70**, 1164 (1998).
- A. Daridon, W. Thronset, I. Liau, K. Farrell, F. Tseng, S. Javadi, and I. Manger, in *Proc. of the Micro TAS Symposium (micro TAS'02)*, edited by Y. Baba, S. Shoji, and A.V.D. Berg (Kluwer Academic Publishers, Nara, Japan, 2002), p. 31.
- K. Handique, D.T. Burke, C.H. Mastrangelo, and M.A. Burns, *Anal. Chem.* **72**, 4100 (2000).

- Y. Huang, N. Chen, J. Bominski, and B. Rubinsky, in *Proceedings of IEEE The Sixteenth Annual International Conference on Micro Electro Mechanical Systems 2003 (MEMS'03)* (IEEE, Kyoto, Japan, 2003), p. 403.
- Y. Jimbo, H.P.C. Robinson, and A. Kawana, *IEEE Trans. on Biomed. Eng.* **40**, 804 (1993).
- S.N. Krylov and N.J. Dovichi, *Electrophoresis* **21**, 767 (2000).
- N. Manaresi, A. Romani, G. Medoro, L. Altomare, A. Leonardi, M. Tartagni, and R. Guerrieri, in *Proceedings of IEEE International Solid-State Circuits Conference 2003 (ISSCC 2003)* (IEEE, San Francisco, USA, 2003), p. 1.
- M. Ozkan, M. Wang, C. Ozkan, R. Flynn, A. Birkbeck, and S. Esener, *Biomedical Microdevices* **5**(1), 61 (2003).
- U. Srinivasan, M.R. Houston, R.T. Howe, and R. Maboudian, *IEEE Journal of Microelectromechanical Systems* **7**, 252 (1998).
- H. Thielecke, T. Stieglitz, H. Beutel, T. Matthies, H.H. Ruf, and J.-U. Meyer, *IEEE Eng. Med. And Biol.* **18**, 48 (1999).
- W. Tong and E.S. Yeung, *J. of Chromatography B* **689**, 321 (1997).
- J.-H. Tsai and L. Lin, in *Technical Digest of the 11th International Conference on Solid-State Sensors and Actuators (Transducers'01)* (IEEE, Munich, Germany, 2001), p. 966.
- A.R. Wheeler, A.M. Leach, and R.N. Zare, in *Proc. of the Micro TAS Symposium (micro TAS'02)*, edited by Y. Baba, S. Shoji, and A.V.D. Berg (Kluwer Academic Publishers, Nara, Japan, 2002), p. 802.